Biomedicine & Pharmacotherapy 111 (2019) 414–426

Contents lists available at ScienceDirect

Biomedicine & Pharmacotherapy

journal homepage: www.elsevier.com/locate/biopha

# Synthesis, characterization, theoretical studies and biological (antioxidant, anticancer, toxicity and neuroprotective) determinations of a copper(II) complex with 5-hydroxytryptophan

Juan J. Martínez Medina[a], Luciana G. Naso[b], Ana L. Pérez[c], Alberto Rizzi[c], Nora B. Okulik[a], María Valcarcel[d], Clarisa Salado[d], Evelina G. Ferrer[b], Patricia A.M. Williams[b,*]

[a] Universidad Nacional del Chaco Austral, Comandante Fernández, 755 - CP: 3700, Presidencia Roque Sáenz Peña, Chaco, Argentina
[b] CEQUINOR, CONICET/CICPBA/UNLP, Facultad de Ciencias Exactas, Universidad Nacional de La Plata, Bv. 120 Nº 1465, 1900 La Plata, Argentina
[c] Departamento de Física, Facultad de Bioquímica y Ciencias Biológicas, Universidad Nacional del Litoral, Ciudad Universitaria-Paraje El Pozo, 3000 Santa Fe, Argentina
[d] Innoprot SL, Edificio 502-P1- Parque Tecnológico, 48160, Derio, Spain

ARTICLE INFO

*Keywords:*
5-hydroxytryptophan copper(II) complex (Cu5HTP)
Neuroprotective action
Anticancer
Antioxidant
Toxicological assays

ABSTRACT

5-Hydroxy-L-tryptophan (5-HTP) is a serotonin pathway metabolite of L-tryptophan in the brain. In the knowledge that the biological properties of some compounds can be modified upon metal complexation, a new solid metal complex, [Cu(5-hydroxytryptophan)$_2$].$H_2O$ (Cu5HTP), has been synthesized and characterized to analyze the modification of some biological properties. The conformational investigations (optimized in gas phase at B3LYP/6-311G** theory level) suggest the coexistence of two conformers of Cu5HTP with *cis*- and *trans*- arrangements of the amino acids in the equatorial plane. The *trans*- Cu5HTP1 complex is the most stable conformer. The complexation led to an enhancement of the antioxidant properties of the ligand. The metal complex also improved the anticancer behavior of the ligand (tested in cancer cell lines derived from human lung (A549), cervix (HeLa) and colon (HCT-116)). It did not show toxicity against either the non-malignant human lung fibroblast (MRC-5) cell line or *Artemia salina* and did not behave as mutagenic agent (Ames test). Cellular reactive oxygen species production may be one of the possible mechanisms of action. Besides, the metal complex exerted neuroprotective action on cortical neurons from embryonic 18 days rats exposed to glutamate.

## 1. Introduction

5-Hydroxy-L-tryptophan (5-HTP) is a serotonin pathway metabolite of L-tryptophan in the brain that controls the concentration of serotonin, and therefore plays a significant role in the serotonin pathway. Besides, 5-HTP is a naturally occurring aromatic amino acid present in the seeds of the African plant *Griffonia simplicifolia* and has been described as an antioxidant agent [1]. Oxidative stress is caused by the reaction of chemically aggressive oxygen species with biomolecules and contributes to the development of some diseases. In plants, phenolic compounds and carotenoids constitute the major tissue-protecting antioxidants. Much less is known on antioxidant agents from animals. The intertidal sponge which survives under intense sunlight, *Hymeniacidon heliophila,* contains the antioxidant 5-HTP as major constituent. Other known antioxidants such as flavonoids, carotenoids or tocopherol derivatives were absent. Both the oxidation potential and the concentration of 5-HTP in *H. heliophila* correspond to the values observed for flavonoids being the major antioxidants in plants [2]. Fig. 1 shows the molecular structure of 2-amino-3-(5-hydroxy-1H-indol-3-yl) propanoic acid (5-HTP).

Copper is an essential dietary nutrient for humans and other mammalian species. The involvement of copper in human diseases has been described from a medicinal-chemical and a biochemical view focusing on the molecular physiology of Cu transport. It is also now clear that high or low body copper levels lead to severe pathological consequences, as observed in Wilson and Menkes diseases. Several well-

*Abbreviations:* 5-HTP, 5-Hydroxy-L-tryptophan; AAPH, 2,2-azobis (2- amidinopropane) dihydrochloride; Cu5HTP, [Cu(5-hydroxytryptophan)2].H2O; DMEM, Dulbecco's Modified Eagle's Medium; DPPH, 1,1-Diphenyl-2-picrylhydrazyl; FBS, Fetal bovine serum; H2DCFDA, 2′,7′-dichlorodihydrofluorescein diacetate; LDH, lactate dehydrogenase; MI, Mutagenic index; MIC, Minimum inhibitory concentration; MK801, ((+)-5-methyl-10,11-dihydro-5H-dibenzo(a,d)cyclo-hepten-5,10-imine); MTT, 3-(4,5-dimethylthiazol-2-yl)-2,5diphenyltetrazolium bromide; NAC, N-acetyl-L-cysteine; NMDA, N-methyl-D-aspartate; NBT, Nitroblue tetrazolium; PBS, Phosphate-buffered saline; PMS, Phenazine methosulfate; ROS, Reactive oxygen species

* Corresponding author.
*E-mail address:* williams@quimica.unlp.edu.ar (P.A.M. Williams).

https://doi.org/10.1016/j.biopha.2018.12.098
Received 20 September 2018; Received in revised form 18 December 2018; Accepted 19 December 2018

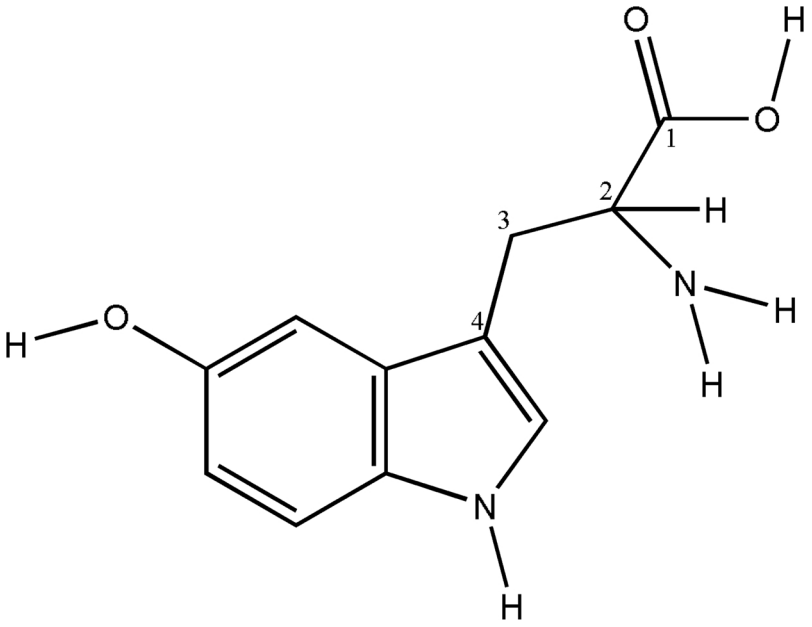


**Fig. 1.** Structure of 2-amino-3-(5-hydroxy-1H-indol-3-yl)propanoic acid (5-HTP).

established symptoms of copper deficiency are related to alterations in the activity of copper-dependent enzymes [3]. The excess of this essential metal produced oxidative stress and the serum and tumor copper levels were elevated in cancer patients in comparison with healthy ones [4]. Copper ions are bound to ceruloplasmin, albumin and other proteins. The copper redox capabilities and complexation potential makes it indispensable for many cellular functions.

In many cases metal coordination leads to an improvement of the pharmacological activities of the ligands and synergistic effects involving both metal and the ligands have been reported. The organic ligands could neutralize the electric charge of Cu(II), increase the lipophilicity of the complex, intercalate to DNA and/or interact with different proteins. The use of copper complexes in medicine, and their potential use as antimicrobial, antiviral, anti-inflammatory, antitumor agents, enzyme inhibitors, has been reported during the last decades. The complexes that showed different size, charge, electron affinity and ability for adduct formation, could interact directly with proteins and DNA, or indirectly producing reactive oxygen species (ROS) that attack and degrade biomolecules [5].

We herein have investigated and characterized a new solid copper complex [Cu(5-hydroxytryptophan)$_2$]·$H_2O$, Cu5HTP. Previous studies on the interaction of 5-HTP with Cu(II) in solution have been performed by fluorescence spectroscopy [6] and stability determinations [7]. Herein, we have prepared the solid complex which was characterized by physicochemical determinations and the geometrical parameters and IR-vibrational assignments have been determined by computational methodologies.

To determine if the metal enhances the antioxidant activity of 5-HTP, the *in vitro* antioxidant behavior of the compounds against DPPH$^{\bullet}$ (1,1-diphenyl-2-picrylhydrazyl) radical and the reactive oxygen species (ROS) superoxide, hydroxyl and peroxyl has been measured. For the determination of the biological effects of the metal complexes it is crucial to assess the effects of the metal and the ligand under the same experimental conditions. As far as we know, the biological effects of metal complexes of 5-HTP have not been reported. Considering that ROS can damage DNA and induced mutagenesis, we have initially determined the anticancer effects and cellular ROS production on different cancer cell lines of the copper(II) cation, 5-HTP and Cu5HTP. We have selected herein human lung cancer A549, human cervical cancer HeLa and human colon cancer HCT-116 cell lines for the *in vitro* anticancer determinations and cellular ROS production [8]. Lung cancer is the primary cause of cancer-associated mortality in males and females worldwide and although there are chemotherapeutic treatments, the prognosis remains poor. It has been established that 90% of cases of lung cancer belong to non-small cell lung cancer (NSCLC). Cervical cancer constitutes the second most common cancer in women after breast cancer, and the infection with one of the types (mainly types 16 and 18) of carcinogenic human papilloma virus (HPV) is associated with high risk of cervical cancer. Colorectal cancer (CRC) is the third most commonly diagnosed cancer in humans. Importantly, treatment of lung fibroblast (MRC-5) cell line has also been tested to determine any significant change in non-malignant human cells. The anticancer studies were coupled with the evaluation of the mutagenicity and acute toxicity of all compounds.

Neurodegenerative diseases such as Alzheimer's, Parkinson's, multiple sclerosis and amyotrophic lateral sclerosis (ALS) are a group of neurological conditions characterized by the loss of neuronal populations in the brain and/or spinal cord. Cognitive impairment, speech difficulties and motor dysfunction are some of the symptoms that can present these disorders [9]. As mentioned above, the synthesis of 5-HTP from L-tryptophan is the first step of the biosynthesis of the neurotransmitter 5-hydroxytryptamine (5-HT) or Serotonin. Supplementation with 5-HTP is hypothesized to normalize serotonin synthesis, crossing the blood-brain barrier and increasing central nervous system synthesis of serotonin. In addition to depression treatment the administration of the amino-acid could be effective in the treatment of a variety of physiological and pathological functions such as insomnia and chronic headaches [10]. Glutamate is the predominant excitatory neurotransmitter in primary perception and cognition in the brain. It is released by presynaptic cells and acts on N-methyl-D-aspartate (NMDA), α-amino-3-hydroxy-5-methyl-4-isoxazolepropionic acid (AMPA), and kainite (KA) receptors producing an excitatory response. When excessive amounts of glutamate are released or when glutamate clearance is insufficient, neuronal death will result in a process with an excessive activation of neuronal amino acid receptors known as excitotoxicity [11,12]. Hence, the glutamate excitotoxicity has been associated to various incurable diseases of the brain including Alzheimer's [13] with median survival of three years, affecting 5.4 people per 100,000 populations over year [14]. Disease-modifying therapy that prevents or slows disease progression is still lacking, therefore there is an urgent need to develop new therapies of neuroprotection against glutamate toxicity. The reported neuroprotective effect exerted by the amino acid

taurine *via* anti-apoptosis in hypoxic-ischemic brain injury in neonatal rats [15] is an example of the neuroprotective action of some amino acids. In addition to the anticancer effects of the compounds we have examined herein their potential neuroprotective effect by means of the study of the signaling pathway in an established *in vitro* model of central nervous system (CNS) injury induced by glutamate. The protocol uses cortical neurons from embryonic 18 days rats and screened the neuroprotective action of compounds by measuring cell counting, lactate dehydrogenase release, caspase 3/7 activation and neurite outgrowth of each compound.

## 2. Materials and methods

### 2.1. Materials

All chemicals used were of analytical grade. Copper(II) chloride dihydrate ($CuCl_2{\cdot}2H_2O$), Copper(II) acetate monohydrate ($Cu(CO_2CH_3)_2{\cdot}H_2O$), para-nitrophenyl phosphate (p-NPP), solvents and all the other analytical grade chemicals used were purchased from Merck. 5-hydroxytryptophan ($C_{11}H_{12}N_2O_3$) was obtained from Xi'an App-Chem Bio(Tech) Co. Ltd. The growth medium (Mueller Hinton Broth and Mueller Hinton Agar) was purchased from Brithania. Elemental analysis for carbon, nitrogen and hydrogen was performed using a Carlo Erba EA1108 analyzer. A Shimadzu system (model TG-50), working in an oxygen flow of 50 mL.min$^{-1}$ and at a heating rate of 10 °C.min$^{-1}$ has been used for the thermogravimetric analysis. Sample quantities ranged between 10 and 20 mg. UV–vis and diffuse reflectance spectra (MgO as a standard) were recorded with a Shimadzu 2600/2700 spectrophotometer. Infrared spectra were measured with a Bruker IFS 66 FTIR spectrophotometer from 4000 to 400 cm$^{-1}$ using the KBr pellet technique. X-band CW-EPR spectra of powdered samples were obtained at room temperature and 120 K on a Bruker EMX-Plus spectrometer, equipped with a rectangular cavity with 100 kHz field modulation. X band EPR spectra of frozen DMSO solutions were recorded at 120 K. EPR spectra were simulated with the EasySpin toolbox based on MATLAB [16]. The molar conductance of the complex was measured on a Conductivity TDS Probe - 850084, Sper Scientific Direct, using $1 \times 10^{-3}$ M DMSO solution.

### 2.2. Synthesis of [Cu(5-hydroxytryptophan)$_2$]·$H_2O$, Cu5HTP

The ligand 5-hydroxytryptophan (1 mmol) was dissolved in distilled water (30 mL) by heating and stirring. After cooling, an aqueous solution of $Cu(CO_2CH_3)_2$ (0.5 mmol, 5 mL) was added to the ligand solution under stirring during 5 min. The light blue precipitate was separated by filtration, washed three times with distilled water and dried in an oven at 60 °C (see Scheme 1). The same product was obtained using $CuCl_2$ instead of the acetate salt and adjusting the pH value to 5 by addition of 1 M NaOH solution.

The solid product was characterized as [Cu(5-hydroxytryptophan)$_2$]·$H_2O$ (Cu5HTP). Anal. calc. for $C_{22}H_{24}N_4O_7Cu$: C 50.8, H 4.6, N 10.8%. Found: C 50.7, H 4.5, N 10.8%. Thermogravimetric analysis (oxygen atmosphere, 50 mL/min): The complex starts decomposing gradually till it attains the temperature at 100 °C which corresponds to 1 mol of hydrated water ($\Delta\omega_{calc}$ = 3.5%, $\Delta\omega_{exp}$ = 3.5%) in a single step process indicated by an endothermic peak. At 800 °C the weight loss (84.7%, calc.; 85.0%, exp.) represents the formation of CuO that was characterized by FTIR spectroscopy. Diffuse reflectance spectrum: 360 nm (sh), 615 nm. UV–vis spectrum ($\lambda_m$, 603 nm; ε, 94.2 M$^{-1}$ cm$^{-1}$; DMSO).

### 2.3. Computational methodology

Since suitable single crystals for structural determinations could not be obtained, the geometrical parameters and the vibrational determinations and assignments of Cu5HTP were studied by computational methodologies. Theoretical calculations were performed using tools from density functional theory (DFT) [17] as implemented in the GAUSSIAN 09 program package [18]. The optimization procedures were carried out using the Beck three-parameters hybrid exchange-correlation functional, known as B3LYP [19] using the 6–311 G basis set [20] reached by adding polarization functions.

The crystallographic data of 5-HTP [21] was used to build the Cu5HTP complex. A conformational investigation of Cu5HTP with a square-planar $CuN_2O_2$ coordination geometry (with two molecules of the N,O-donor amino acid) was performed taking into account the *cis* and *trans* conformations of the aliphatic nitrogen and a carboxylate oxygen in the coordination sphere ($CuN_2O_2$). Besides, the rotation around C2-C3 bond, defined as the dihedral angle C1-C2-C3-C4 (see Fig. 1), was considered in the established models. This dihedral angle configures the relative position of the plane of 5-HTP-rings system with respect to the planar coordination sphere ($CuN_2O_2$). These calculations were performed in gas phase combining different functionals (SVWN and B3LYP) with different basis sets (3–21 G, 6–31 G, 6–31 G** and 6–311 G**). For the resultant structures of the conformational search optimized at B3LYP/6-311** theory level, the harmonic vibrational frequencies were calculated at the same level of theory. These calculations are necessary to confirm the presence of true minimum energy structures, as well as to perform thermodynamic corrections (that are included in all electronic energies reported) and to assign the theoretical vibrational spectra. The IR frequencies were analyzed by means of Potential Energy Distribution (PED%) calculation using Vibrational Energy Distribution Analysis (VEDA 4) program [22].

### 2.4. Antioxidant properties

The experimental conditions for the antioxidant determinations were set according to previous reports [23]. The superoxide dismutase (SOD) activity was examined indirectly using the nitroblue tetrazolium (NBT) assay. The indirect determination of the activity of 5-HTP and the Cu5HTP was assayed by their ability to inhibit the reduction of NBT by the superoxide anion generated by the phenazine methosulfate (PMS) and reduced nicotinamide adenine dinucleotide (NADH) system. The concentration of compound that gave a 50% inhibition ($IC_{50}$) was obtained from the plot of the percentage of inhibition *versus* the negative log of the concentration. The capacity to scavenge hydroxyl radicals (generated by the ascorbate-iron-$H_2O_2$ system) has been determined by the measurement of the extent of deoxyribose degradation by hydroxyl radical with the thiobarbituric acid method. The inhibition of peroxyl radical was measured by generation of the radicals by the thermal decomposition of 2,2-azobis (2-amidinopropane) dihydrochloride (AAPH). The delay of pyranine consumption (lag phase)

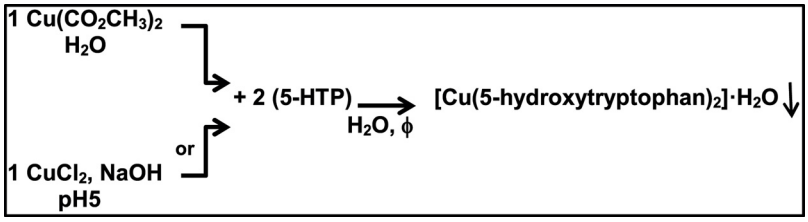


**Scheme 1.** Schematic representation of the reaction of synthesis of Cu5HTP.

was calculated as the time before the consumption of pyranine started (notable reductions in absorbance). The antiradical activity of the compounds was also measured in terms of their capacity to scavenge DPPH$^{\bullet}$ (1,1-diphenyl-2-picrylhydrazyl) radicals. Each experiment was performed in triplicate and at least three independent experiments were evaluated in each case.

### 2.5. Anticancer effects

#### 2.5.1. Cell culture

Human lung cancer cell line A549, human cervical cancer cell line HeLa and human colon cancer cell line HCT-116 were maintained at 37 °C in a 5% carbon dioxide atmosphere using DMEM supplemented with 100 U/mL penicillin, 100 μg mL$^{-1}$ streptomycin and 10% (v/v) fetal bovine serum as the culture medium. Human fetal lung fibroblasts (MRC-5 cell line) were grown as monolayer in DMEM supplemented with 20% fetal bovine serum. When 70–80% confluence was reached, cells were subcultured using TrypLE™ from Gibco (Gaithersburg, MD, USA) and free phosphate buffered saline (PBS) (11 mM $KH_2PO_4$, 26 mM $Na_2HPO_4$, 115 mM NaCl, pH 7.4). For the experiments, cells were grown in multi-well plates. When cells reached 70% confluence, the monolayers were washed twice with DMEM and then incubated with the different compounds.

#### 2.5.2. Cell viability assay

For the MTT (3-(4,5-dimethylthiazol-2-yl)-2,5diphenyltetrazolium bromide) assay, A549, HeLa, HCT-116 and MRC-5 cells were seeded at a density of $1 \times 10^5$ per well in 48 well plates, grown overnight and treated with different concentrations of 5-HTP, Cu5HTP or copper(II) cation in FBS free medium. Dimethyl sulfoxide (DMSO) has been used as the dissolution vehicle to yield a maximum final concentration of 0.5% in each well (Sigma-Aldrich, St. Louis, MO). After 24 h incubation at 37 °C, 100 mg MTT (Sigma-Aldrich, St. Louis, MO) per well was added and then incubated for 2 h. By cellular reduction of MTT formazan products were generated. Formazan was dissolved in isopropyl alcohol/HCl (cancer cell lines) or DMSO (normal cell line) and the optical density was measured at 560 nm. All experiments were performed in triplicate. Data were presented as percentage of cell viability (%) of the treated group with respect to the untreated cells (control) in which the viability is assumed to be 100%.

#### 2.5.3. Cell morphology

To further evaluate the altered morphology induced by the copper complex and the metal center, cells were grown in six well per plates and incubated overnight with fresh serum-free DMEM without (control) or with different concentrations of the complex. The monolayers were subsequently washed twice with PBS, fixed with methanol and stained with 1:10 dilution of Giemsa for 10 min. Next, they were washed with water and the morphological changes were examined by light microscopy.

#### 2.5.4. ROS measurements

Intracellular reactive oxygen species (ROS) generation in the A549, HeLa, HCT-116 cell lines was measured by oxidation of 2′,7′-dichlorodihydrofluorescein diacetate ($H_2$DCFDA) to 2′,7′-dichlorofluorescein (DCF). Briefly, 48-well plates were seeded with $5 \times 10^4$ cells per well and allowed to adhere overnight. Then, different concentrations of 5-HTP, Cu5HTP and copper(II) cation were added for 2 and/or 24 h. Afterwards, media was removed and cells were loaded with 10 μM $H_2$DCFDA diluted in clear media for 30 min at 37 °C. Media were separated and the cell monolayers rinsed with PBS and lysated into 1 mL 0.1% Triton-X100. The cell extracts were then analyzed for the oxidized product DCF by fluorescence spectroscopy (excitation wavelength, 485 nm; emission wavelength, 535 nm), using a Perkin-Elmer LS 50B spectrofluorometer.

### 2.6. Toxicological assays

For the determination of the acute toxicity of $CuCl_2$, 5-HTP and the Cu5HTP in brine shrimp, eggs of *A. salina* were incubated in a hatching chamber with artificial seawater at 20–30 °C (One liter of seawater contains: NaCl, 23 g; $MgCl_2.6H_2O$, 11 g; $Na_2SO_4$, 4 g; $CaCl_2.2H_2O$, 1.3 g; KCl, 0.7 g). The pH was adjusted to 9.0 using $Na_2CO_3$ to avoid risk of death to the *Artemia* larvae by the decrease of pH during incubation [24]. After 24 h, the larvae (nauplii) were extracted and counted using a micropipette. Six concentrations of the compounds (in triplicate) were tested in order to determine the dose-response relationship and negative (distilled water) and positive ($K_2Cr_2O_7$) controls were used. The selected concentrations tested were in the order of those used for the anticancer determinations. The wells containing the sample and larvae of brine shrimp, including the control groups, were filled to a total volume of 100 μl with artificial seawater. After 24 h, live larvae were counted and the median lethal concentration ($LC_{50}$) values were estimated.

Some chemical agents which show mutagenicity can induce cancer. Then, it is useful to study the mutagenic potential of novel drugs. Mutagenicity of the compounds was evaluated by the *Salmonella*/microsome assay that is based on the plate-incorporation method proposed by Maron and Ames [25], using *Salmonella typhimurium* TA98 and *Salmonella typhimurium* TA100. The test strains were obtained from frozen culture and were grown overnight for 12–14 h at 37 °C in Mueller Hinton broth. The different concentrations of $CuCl_2$, 5-HTP and the Cu5HTP (300, 150, 75, 37.5 and 18.8 μg/plate) were added to 2 mL of top agar mixed with 100 μl of bacterial culture ($1–2 \times 10^8$ cells mL$^{-1}$) adding this mixture to a plate with minimal agar. These plates were incubated at 37 °C for 48 h and the number of His + revertant colonies was counted. All experiments were made in duplicate. The Mutagenic index (MI) was calculated as the average number of revertants per plate divided by the average number of revertants per plate from the negative control for each dose.

### 2.7. Neuroprotective signaling pathway

Primary cultures of cortical neurons were prepared from the cerebral cortices of Sprague-Dawley rat fetuses at embryonic day 18. Brains were removed and freed from the meninges, and the tissues were then dissected under a binocular microscope. Neurons were enzymatically dispersed with trypsin 0.2% and DNAsa I 0.04% for 10 min at 37 °C and plated on poly-L-lysine wells with neurobasal medium supplemented with B-27 supplement.

For the experimental assay of excitotoxicity induce by glutamate, cortical neurons from embryonic 18 days rats were plated in poly-L-lysine coated 96-well plates with a density of $3 \times 10^4$ cells per well. Cells were maintained in neurobasal medium supplemented with B-27 supplement for 8 days at 37 °C in a humidified 5% $CO_2$ atmosphere. At day 8, cells were pre-treated with compounds for 1 h in neurobasal medium supplemented with B-27 supplement. After the treatments, cells were washed and returned to compound-free medium for up to 48 h before being subjected to a glutamate excitotoxicity condition where cells were incubated with 100 μM glutamate during 15 min in medium without B-27 supplement. After glutamate exposure, medium was replaced by neurobasal medium supplemented with B-27 factor, and then cells were incubated for an additional 24 h. Some cells were treated as described above with 10 μM MK801 ((+)-5-methyl-10,11-dihydro-5H-dibenzo(a,d)cyclo-hepten-5,10-imine) as positive control of neuroprotection.

The neuroprotective effects were quantified by High Content Assay, which included the following endpoints: plasma membrane integrity, cell number, caspase 3/7 activation and neurite outgrowth. For the determination of the plasma membrane integrity, the supernatants were collected 24 h after treatments and lactate dehydrogenase LDH assay was performed following the instructions of the kit manufacturer. Cell

viability was determined using Hoechst 33342 nucleic acid stain. Cells were stained with 5 μg/mL of Hoechst 33342 dye, washed 3 times and measured at 380 nm/460 nm Ex/Em. This dye allows a sensitive cell number determination by fluorescence microscopy. Caspase 3/7 activation was determined using The CellEvent® Caspase-3/7 Green Detection Reagent which is intrinsically a non-fluorescent peptide that inhibits the ability of the dye to bind to DNA. However, after activation of caspase-3/7 in apoptotic cells, the peptide is cleaved enabling the dye to bind to DNA and produce a bright, fluorogenic response. Cells were stained with 5 μM reagents, washed 3 times and measured at 488 nm/530 nm Ex/Em. This dye allows the direct quantification of apoptotic cells.

Beta-III tubulin staining was determined by immunohistochemistry. Once cells were stained and image with fluorescent dyes, cells were washed with PBS and fixed with 4% paraformaldehyde for 15 min. After the fixation step the samples were washed three times with PBS and permeabilized with PBS + 0.3% triton for 10 min. The samples were then blocked with PBS + Bovine Serum Albumin (BSA) for 30 min and finally anti-tubulin III antibody were added at 1/1000 in PBS + 0.5% BSA for 60 min at room temperature. After three washing steps, the secondary antibodies Alexa 633 were added at 1/100 for 60 min to react against the primary antibody. The samples were then washed three times and measured in the Pathway 855 automated fluorescent microscope. To investigate the role of neurite extension one geometric pattern was employed in this study: neurite average length per neuron. At the end of the assay, cells were firstly simultaneously loaded with fluorescent dyes. After 1 h incubation at 37 °C with the culture media containing the fluorescent probes, cells were imaged using BD Pathway 855, and the attovision analyzer system was employed. Then, cells were fixed for beta-III tubulin staining and imaged again using BD Pathway 855. In order to acquire enough cells for the analysis, nine fields per well were imaged. The 20x objective was used to collect images for the distinct fluorescence channels. Dyes were excited and their fluorescence was monitored at the excitation and emission wavelengths with appropriate filter settings. In the setting up of the procedure, exposure times were adjusted in order to avoid overlapping emission between different probes. The collected images were analysed using a module that allows the simultaneous quantification of subcellular structures, which are stained by different molecular probes and measure the fluorescence intensity associated with predefined nuclear and cytoplasmic compartments.

### 2.8. Statistical analysis

Statistical differences were analyzed using the analysis of variance method (ANOVA) followed by the test of least significant difference (Fisher). Statistical significance was defined as $p < 0.05$.

## 3. Results

### 3.1. Solid characterization of the complex

#### 3.1.1. Vibrational spectroscopy

The tentative assignments for the most important and characteristic vibrational bands of the FTIR spectra for 5-HTP and Cu5HTP (in KBr pellets) are displayed in Table S1. This assignment is based on some previous reports of 5-HTP [26], L-Tryptophan [27] and the Copper(II) L-Tryptophan complexes [28]. The presence of the characteristic stretching and bending, $\nu(NH_3^+)$, $\delta(NH_3^+)$ and $\nu(COO^-)$, bands in the free ligand confirms the existence of 5-HTP in the zwitterionic form at solid state and the broad bands at (2900-2600 $cm^{-1}$ range) indicated that H-bonds operate in the ligand. The vibration modes of the OH group at C-5 appeared in the spectra of both for the ligand and the complex. After complexation and deprotonation, the position of the $\nu_{as}(NH_2)$ and the $\nu_s(NH_2)$ vibration bands supports the involvement of this group in bonding [29]. The participation of the carboxylate group on copper binding was also determined by the shift of the band positions. The antisymmetric and symmetric $COO^-$ stretching vibrations ($\nu_{as}(COO^-)$ and $\nu_s(COO^-)$) assigned to the 5-HTP (zwitterionic form) shifted to lower frequencies upon coordination. The difference $\Delta\nu = \nu_{as}(COO^-) - \nu_s(COO^-)$, used as a criterion to establish the coordination mode of the $COO^-$ group to the metal [30], resulted higher for the complex (232 $cm^{-1}$) than for the ligand (211 $cm^{-1}$), in concordance with a unidentate coordination mode of the carboxylate moiety. These results suggest that the coordination of the copper(II) ion with the 5-HTP ligand most probably took place *via* carboxylate ($COO^-$) and amino ($NH_2$) groups of the aminoacid. This conclusion is supported by solution EPR determinations (see below).

#### 3.1.2. EPR measurements

EPR and NMR spectroscopies are similar techniques but EPR determinations concerned with the magnetically induced splitting of electronic spin states, while NMR focus on the splitting of nuclear spin states. The $^1H$ NMR spectra of paramagnetic metal complexes are not as well resolved as those of corresponding diamagnetic compounds. It is a useful tool in studying the structural properties of Cu(II) coordination compounds in solution, but the slow electronic relaxation of Cu(II) ions usually results in large line widths and poor resolution of the spectra. Furthermore, EPR spectroscopy is a powerful tool in the study of the structures and environments of species that have unpaired electrons like metal ions and organic free radicals. As the electronic analog of NMR spectroscopy that probes the nuclear spin of molecules, it allows the characterization of the geometry and electronic structure of the copper(II) complexes [31]. This is the reason why we have selected this technique to determine the environment and geometry of Cu5HTP complex.

The EPR spectrum recorded for a powder sample of Cu5HTP together with the simulation measured at room temperature is displayed in Fig. S1. The EPR spectrum shows axial g-values ($g_x = g_y = g_\perp = 2.061$, $g_z = g_{//} = 2.226$) typical for a Cu(II) species ($S = 1/2$) in elongated octahedral, square pyramidal, or square planar geometries, where the ground state is the $d_{x2-y2}$ orbital [32]. A similar spectrum was obtained at 120 K (data not shown). No resolved hyperfine structure could be observable. This fact is compatible with the presence of interaction between metal centers (typical of copper centers in an extended lattice), where the exchange interaction collapses the typical 4-lines hyperfine interaction with the Cu(II) nucleus ($I = 3/2$). The low value obtained for $g_{//}$ ($g < 2.4$) is in concordance with a square planar geometry. These data were taken into account in order to perform optimization of the more reliable structure by DFT calculations.

#### 3.1.3. DFT calculations

The conformational and structural analysis of Cu5HTP was carried out without any constrains. The optimization procedures of the different conformers of Cu5HTP were performed employing different functionals combined with different basis sets. Nevertheless, only five structures converged at B3LYP/6-311G** and they are confirmed as minimum energy structures (Fig. S2). The geometrical and energetic aspects of the five conformers are listed in Table S2. The conformers 1 (*trans*) and 2 (*cis*) are the most stable conformers and they have an energetic difference (ΔE) lower than 2 kcal $mol^{-1}$ suggesting the coexistence of both species at room temperature. The relative populations of these two conformers were calculated by the Maxwell-Boltzmann distribution at 298.15 K. The conformers 1 and 2 show relative populations close to 86% and 14%, respectively. These results led us to select the structure of these two conformers in order to study their geometrical and vibrational aspects.

The metal center in the optimized structure of Cu5HTP1 presents a square-planar $CuN_2O_2$ environment with a *trans* arrangement of the amino acids in the equatorial plane, involving the terminal amino and carboxylate groups of two molecules of 5-HTP. On the other hand, the optimized structure of Cu5HTP2 indicates that this complex have the

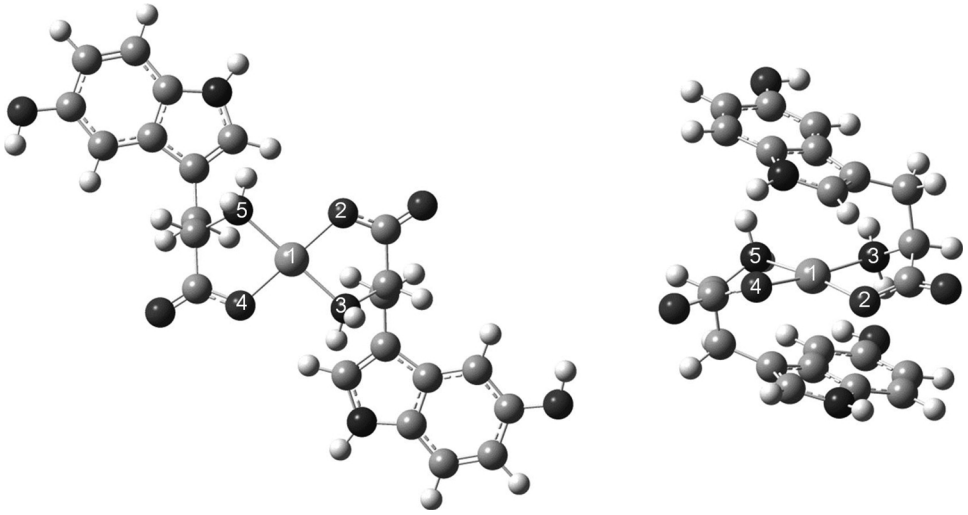


**Fig. 2.** Geometry of the Cu5HTP1 (left) and Cu5HTP2 (right) complexes optimized at the B3LYP/6-311G** level of theory. The white ball represents H atom, the black ball represents N atom, the gray ball represents O atom, the light gray ball represents C atom and the big light gray ball represents Cu atom. The atoms around the copper (atom 1) are numbered.

**Table 1**
Selected bond lengths (Å) and angles (°) around copper in the Cu5HTP1 and Cu5HTP2 complexes calculated at B3LYP/6-311G** theory level.

| Bond Lenghts[a] | Cu5HTP1 | Cu5HTP2 | Bond Angles[a] | Cu5HTP1 | Cu5HTP2 |
|---|---|---|---|---|---|
| Cu(1)-O(2) | 1.904 | 1.937 | O(2)-Cu(1)-N(3) | 84.44 | 81.99 |
| Cu(1)-O(4) | 1.904 | 1.937 | O(4)-Cu(1)-N(5) | 84.44 | 81.99 |
| Cu(1)-N(3) | 2.010 | 2.042 | O(2)-Cu(1)-N(5) | 95.68 | 173.24 |
| Cu(1)-N(5) | 2.010 | 2.042 | O(4)-Cu(1)-N(3) | 95.68 | 173.24 |
| | | | O(2)-Cu(1)-O(4) | 175.44 | 96.78 |
| | | | N(3)-Cu(1)-N(5) | 176.97 | 100.00 |

[a] For the numbering of the atoms see Fig. 2.

Cu(II) ion in a distorted square-planar geometry with a *cis* arrangement of the aliphatic nitrogen and a carboxylate oxygen of the $CuN_2O_2$ environment. The Cu5HTP1 complex (*trans*) is the most stable conformer, in agreement with previous reports of the parent aminoacid tryptophan/Cu(II) complex, $Cu(Trp)_2$ [28]. Fig. 2 shows the optimized geometry of the Cu5HTP1 and Cu5HTP2 complexes at the B3LYP/6-311G** level of theory, including hydrogen atoms and numbers of the atoms around the copper in the coordination sphere. Representative bond lengths and angles around the copper atom in both conformers are depicted in Table 1.

The experimental and the theoretical FTIR spectra of the Cu5HTP complex, calculated at the same level of theory employed in the optimization procedure (B3LYP/6-311G**), are shown in Fig. S3. The theoretical FTIR spectra have been built weighting the spectra of Cu5HTP1 (86%) and Cu5HTP2 (14%), attending the relative population percentage of these two conformers calculated by the Maxwell-Boltzmann equation (see Table 1). The results of our simulation employing different scaling factors [33] for different regions of the spectrum (frequencies < 1000 = 1.0119 and frequencies > 1000 = 0.9682) are slightly different from the experimental data. Nevertheless, this difference could be explained by the fact that the experimental FTIR spectrum was measured in the solid state in which the structure is subjected to intra and intermolecular interactions such us hydrogen bonding and van der Waals interactions, whereas the calculations for the isolated molecule have been performed in gas phase. In this context, the Potential Energy Distribution (PED) analysis is an indispensable tool for a serious analysis of the vibrational spectra. The analysis of vibrational results was carried out employing VEDA 4 program in order to identify the most important components in each vibrational mode with a description using internal coordinates. The results of PED analysis for Cu5HTP1 and Cu5HTP2 complexes are displayed in Table S3. The contribution percentages of each coupled mode for the same wavenumber are indicated in parentheses.

### 3.2. Solution studies

#### 3.2.1. Electronic spectra

The reported pK values for 5-HTP are: $pK_1$ (−COOH) = 2.65, $pK_2$ ($-NH_3^+$) = 9.63, $pK_3$ (5−OH) = 10.68. The variation of the UV–vis spectra of an aqueous solution of the aminoacid 5-HTP ($5 \times 10^{-5}$ M) *vs.* pH agree with these values (Fig. S4 A). The stability constants for the complexes Cu(HL) and $Cu(HL)_2$ ($\log\beta_1$, 8.61 and $\log\beta_2$,15.76, respectively) have also been reported [7]. It has to be noted that these values were determined by different methods and showed slight deviations. The electronic spectral pattern obtained from aqueous solutions of a mixture of 5-HTP ($1 \times 10^{-4}$ M) and $CuCl_2.2H_2O$ ($5 \times 10^{-5}$ M) at different pH values (Fig. S4C). Working with 100 times concentrated solutions, the visible part of the electronic spectrum of the complex can be detected. The electronic spectra of aqueous solutions of 5-HTP ($1 \times 10^{-2}$ M) and $CuCl_2.2H_2O$ ($5 \times 10^{-3}$ M) at different pH values in the range 400 nm to 1000 nm are shown in Fig. S4D. At pH values lower than 3 the typical spectrum of $[Cu(H_2O)_6]^{2+}$ complex can be observed ($\lambda m$ = 830 nm). Complex formation took place at pH 5–6 ($\lambda m$ = 620 nm). At higher pH values new species and hydrolysis products have been observed. Then, a pH value of 5 has been selected for the synthesis of the complex.

There is a spectrum-structure correlation for copper(II) complexes in aqueous solution that allow the calculation of the absorption maximum (nm) using estimated wavenumber coefficients:

$$\lambda max = 10^3/(\sum_{i=1}^{4} nivi)$$

Considering the Coefficient ($\nu_i$) values for amino nitrogen (0.450) and for carboxylate oxygen (0.353), the visible spectrophotometric $\lambda_{max}$ value for equatorially-coordinated copper(II) complexes in aqueous solution can be estimated. The calculated value of the electronic absorption maximum was 623 nm. This value resembles that of the diffuse reflectance spectrum (615 nm) and is similar, within the experimental error (10 nm), to the value obtained for an aqueous solution at pH 5–6 of 620 nm (see supplementary data), indicating a metal environment of two N and two O atoms in the equatorial plane [34].

#### 3.2.2. EPR spectrum in solution

It is well known [35] that EPR spectra of pure paramagnetic compounds (*i.e.*, systems in which the paramagnetic centers are not diluted) are dominated by interactions between the metal centers and therefore yield little information about the individual centers. In these cases, and to gather information about the spectroscopic properties of the individual metal ion, solution or doped samples spectra have to be taken

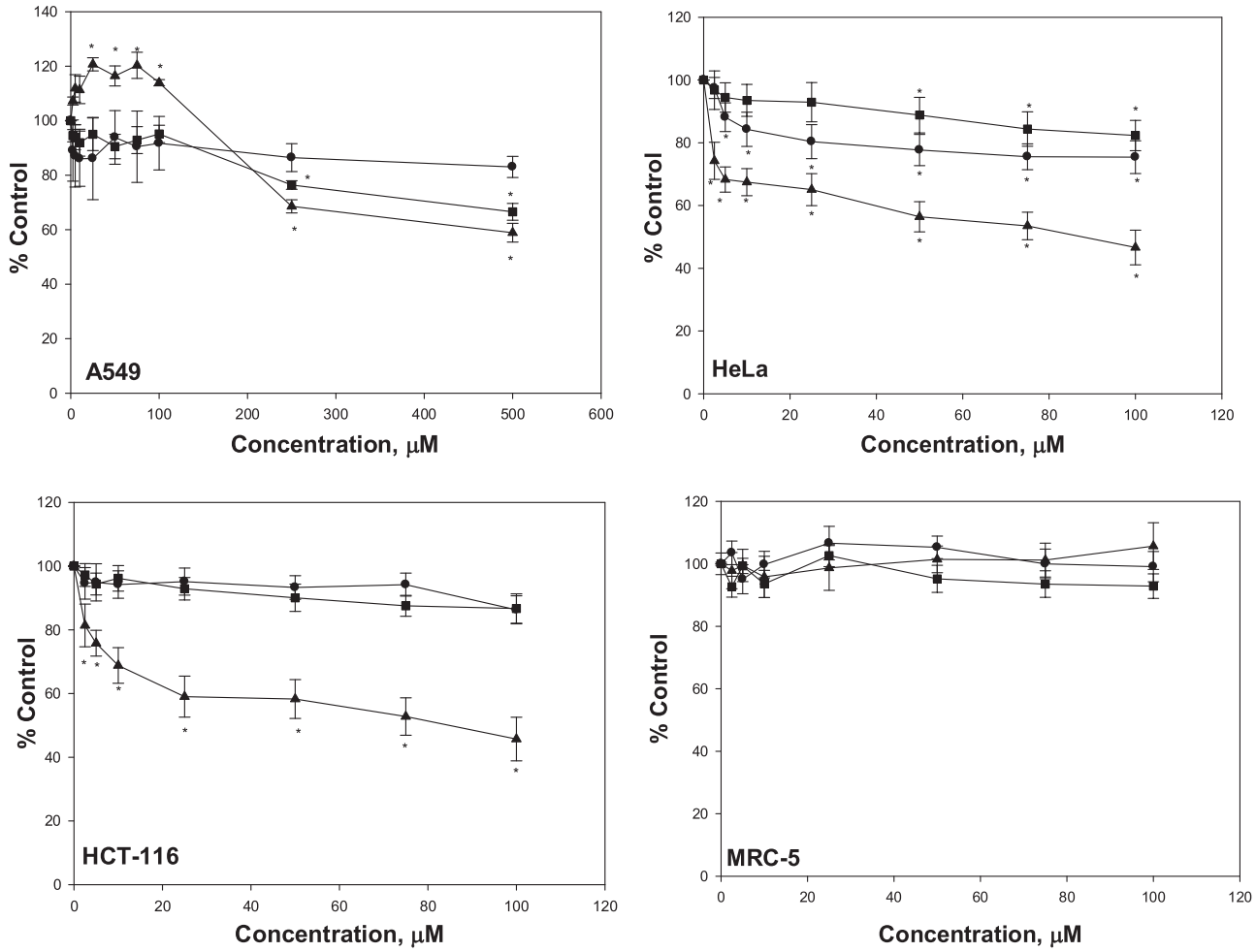


**Fig. 3.** Effects of 5-HTP (circles), Cu5HTP (triangles) and copper(II) cation (squares) on A549, HeLa, HCT-116 and MRC-5 cell line viability. The cell lines were treated with various concentrations of the compounds for 24 h. The results are expressed as the percentage of the control level and represent the mean ± the standard error of the mean (SEM) from three separate experiments (n = 15). * significant values in comparison with the control level ($p < 0.05$).

to avoid the interactions between the metal ions. Because the solid EPR spectrum of the complex showed interactions between the metal centers, the experimental EPR spectrum for a frozen solution of Cu5HTP at 120 K has been measured and the simulation was performed. From Fig. S5 a nearly axial EPR spectrum can be seen ($g_x = 2.058$, $g_y = 2.045$, $g_z = 2.249$) with clearly resolved 4-lines hyperfine structure ($A_x = 12.9$ G, $A_y = 20.6$ G, $A_z = 179.3$ G) due to the interaction of the unpaired electron spin with the Cu(II) nucleus (I = 3/2), results also indicating a $d_{x2-y2}$ ground state and the formation of a single mononuclear species after dissolution. According to the Peisach Blumberg correlation [36], the $A_{//}$ and $g_{//}$ values found in the simulation of the spectrum are compatible with a copper(II) ion in a 2N-2O coordination environment, in line with FTIR results. Furthermore, the frozen solution EPR spectrum shows a five-line super-hyperfine splitting pattern at B = 3265 G ($g \approx 2.068$) (see inset on Figure S5), indicating that there is, besides the interaction with the I = 3/2 of the copper nucleus, an additional hyperfine interaction with two equivalent nitrogen (I = 1) nuclei, tentatively assigned to two N atoms from two 5HTP ligands. As shown in the inset on Figure S5, this N-hyperfine coupling was evaluated to be $a_N \approx 12$ G ($\approx 11.6 \times 10^{-4}$ cm$^{-1}$), compatible with values of $a_N$ found in similar Cu(II) compounds. [37] It is worth to note that this hyperfine coupling was not experimentally observed in all the spectral features, indicating that the linewidth of the different hyperfine components is not the same, which could not be reproduced in our simulation. In any case, the hyperfine interaction attributable to two N atoms is strong evidence that the proposed 2N2O solid state coordination is kept in the DMSO solution.

### 3.2.3. Stability of the complex

The stability of Cu5HTP was measured in DMSO since this solvent has been used as a co-solvent in the biological determinations. To test the stability of the complex upon dissolution in DMSO, its rate of decomposition was spectrophotometrically measured. The complex ($8 \times 10^{-3}$ M) remained stable in a DMSO solution (no appreciable changes were observed in the UV–vis spectra) at least during 1 h (data not shown). The molar conductivity measurement of the complex has been carried out in a 1 mM DMSO solution. The obtained value (11 $\Omega^{-1}$ cm$^2$ mol$^{-1}$) revealed the non-electrolytic nature of the Cu5HTP complex [38], indicating that the complex maintain its structure in solution. This value remains unchanged during 24 h. Hence, by two different experimental determinations it can be stated that the complex did not decompose during the manipulation of the solution for the biological studies.

### 3.3. Antioxidant determinations

The antioxidant properties of 5-HTP and Cu5HTP have been evaluated by means on the capacity of the compounds to scavenge reactive oxygen species (ROS) *in vitro*. In addition, the capacity of the reduction of the concentration of the DPPH$^{\cdot}$ radical has been evaluated for comparative purposes. 5-HTP did not display SOD activity whereas its copper complex improved the capacity of dismutation of the superoxide

anion showing a relevant activity ($IC_{50}$ = 4.8 μM) in comparison with the activities of the $CuCl_2$ ($IC_{50}$ = 3.6 μM) and native SOD ($IC_{50}$ = 0.21 μM) [39] (Fig. S6B). The aminoacid is not a good $OH^{\cdot}$ scavenger and Cu5HTP showed a moderate antioxidant activity against $OH^{\cdot}$ radicals, scavenging *ca.* 43% of the radicals at a 75 μM concentration (Fig. S6C). Both 5-HTPand Cu5HTP were able to scavenge 89.4 and 91.3% of the $DPPH^{\cdot}$ radicals at 25 μM, respectively (Fig. S6D).

The 5-HTP aminoacid is able to prevent damage of biochemically important molecules at physiological pH value. It acted as a naturally occurring, endogenous antioxidant in marine organisms [2]. Our results for 5-HTP showed that the amino acid behaved as a good scavenger for reactive oxygen species (except superoxide anion) in agreement with previous results [40] and the $DPPH^{\bullet}$ radical-scavenging activity indicated that 5-HTP has excellent hydrogen-donating ability. It has also been reported that the ligand did not act as a prooxidant agent in the linoleic acid/β-carotene-bleaching system, effect similar to that of the synthetic antioxidant Trolox. Copper complexes with biologically active molecules are being prepared as synthetic SOD mimics because of the ability of copper to participate in redox reactions and to improve the own limitations of the enzyme (lack of oral bioavailability, high molecular weight and low stability). Likewise, it has been reported that the greater is the distortion in the geometry of the complexes the enhanced effect on SOD activity [41]. Herein it can be seen that the copper complexation enhanced the antioxidant activity of 5-HTP against all radicals, and particularly, it was able to improve the scavenging action against superoxide anion, as expected.

### 3.4. Anticancer effects

#### 3.4.1. Cell viability

Cytotoxic effects of 5-HTP, Cu5HTP and copper(II) cation on malignant cell lines derived from human lung (A549), cervical (HeLa) and colon (HCT-116) cancer are depicted in Fig. 3. The activity of the compounds on non-malignant human lung fibroblast (MRC-5) cell line was evaluated to demonstrate their selectivity towards malignant cells. The natural aminoacid 5-HTP showed low cytotoxicity against the tested cancer cell lines being the $IC_{50}$ values > 100 μM. In the A549 cell line, Cu5HTP displays a biphasic behavior, inducing an increase in cell viability up to 100 μM and a cytotoxic effect at high concentrations (*ca.* 40% inhibition at 500 μM). However, in both HeLa and HCT-116 cell lines the complex inhibited the cell viability in a dose-response manner (*ca.* 50% inhibition at 100 μM). In agreement with previously published assays, our results showed that copper(II) cation displayed insignificant *in vitro* cytotoxicity [42].

A reasonable way of assessing anticancer activity *in vitro* is to test the ability of drugs to kill cancer cells without significantly affecting nonmalignant cells. To determine if the compounds were able to kill cancer cells selectively at concentrations that do not significantly affect the healthy cells, the MRC-5 cell line has been selected. From Fig. 3 it can be seen that the compounds did not show toxicity against the fibroblast normal line. The results for $CuCl_2$ agree with previous determinations [43]. Moreover, these compounds did not show either toxicity by the *Artemia salina* test or mutagenic effects by the Ames assay (see below).

#### 3.4.2. Morphological changes

An inverted microscope was used to examine cell morphology alterations by Giemsa staining (Fig. 4A and B). The morphological changes after addition of Cu5HTP are shown in Fig. 4A. The analysis for A549 cells showed the expected pebble-like shape, close cellular adhesion and clear cell boundaries [44]. Upon 500 μM Cu5HTP treatment morphological changes such as cell shrinkage and pyknotic nuclei can be observed. Untreated HeLa cells showed typical rhomboid-tetrahedral shape and pleomorphic nuclei [45] and after Cu5HTP treatment, especially at 100 μM, shrinkage, nuclear condensation elongated lamellipodia and many detached cells can be observed. Defined nuclei and presence of nucleoli is the typical morphology of HCT-116 cells [46]. Morphological changes like condensed nuclei and cell shrinkage were observed when 100 μM of the complex was added. In all three cases, the decrease in the number of cells is in agreement with the MTT assay. To discard that the morphological changes of immortalized cell lines treatment could be due to the dissociation of the complex and the release of copper ions, a control experiment post $CuCl_2$ incubation has been performed (Fig. 4B). It can be observed that the metal, at concentration 100 μM, did not affect the morphology (shape and size) of the nucleus and the cytoplasm in the three cell lines. In the HeLa cell line a slight decrease in the number of cells was detected. The results are in agreement with the observations in the cell viability test. please change the color of the table from red to black

#### 3.4.3. Intracellular ROS production

The mechanism of action of many chemotherapeutic agents is based on the reactive oxygen species (ROS) generation. It is known that cancer cells possess certain characteristics different from the normal cells such as increase in metabolic rate, ROS generation and decrease in ROS elimination processes [47]. While high levels of ROS can induce damage in macromolecules such as lipids, proteins and DNA, low levels can act as cellular signaling messengers [48]. To investigate the possible production of ROS in A549, HeLa and HCT-116 cell lines, cells were incubated with different concentrations of the compounds during 24 h. For the A549 cell line it can be observed that there are no differences with respect to the control working with concentrations up to 100 μM (Fig. 5). At concentrations higher than 250 μM the compounds produced a slight decrease in ROS production. Conversely, 5-HTP did not show differences with the control cells. The behavior on ROS production of both 5-HTP and $CuCl_2$ is similar in HeLa and HCT-116 cell lines, Fig. 5, generating a slight increment in ROS levels. On the other hand, Cu5HTP induced an increment in intracellular ROS levels in both cells line in a dose-dependent manner (*ca.* 160–170 % at 100 μM). These results are in agreement with the cell killing effects of the metal complex in the human cervical and human colon cancer cell lines.

Considering that in the human lung cancer cell line the compounds produced a reduction in cell viability (at concentrations > 100 μM) associated with a decrease of intracellular ROS levels, we have performed the experiment of ROS measurements reducing the incubation time. The A549 cell line was incubated with 250 and 500 μM concentrations of the compounds for 2 h. An increase in ROS production in a dose-dependent manner was observed for $CuCl_2$ and Cu5HTP (Fig. 6) showing that ROS could be initiated at shorter times and that it is significantly associated with the cell death observed at 24 h incubation (Fig. 3). At concentrations lower than 100 μM, no cellular ROS production was detected.

Our results showed that the complex improves the activity of the natural aminoacid on the three tested tumor cell lines without affecting the normal fibroblast viability, being the oxidative stress one of the possible mechanisms of action.

### 3.5. Toxicological assays

Once the lack of toxicity of the compounds in the normal cell line has been determined, the study of their possible toxic effects can be extended through the *Artemia salina* L. test. This assay is useful for the screening of novel drugs in order to predict their toxicity and has shown a good correlation ($r = 0.85$ $p < 0.05$) with the assays in mice, suggesting that the brine shrimp bioassay is a useful alternative model [49]. The mortality of brine shrimp produced by $Cu^{2+}$ has previously been reported [50] and is slightly different from our data ($LC_{50}$ = 89.76 μg $mL^{-1}$). These differences could be due to the different methodologies, experimental conditions (especially the copper salt and the composition of sea water used) and the strain of eggs. On the contrary, 5-HTP and the Cu5HTP complex did not produce dead nauplii at the tested concentrations, thus suggesting that these compounds did

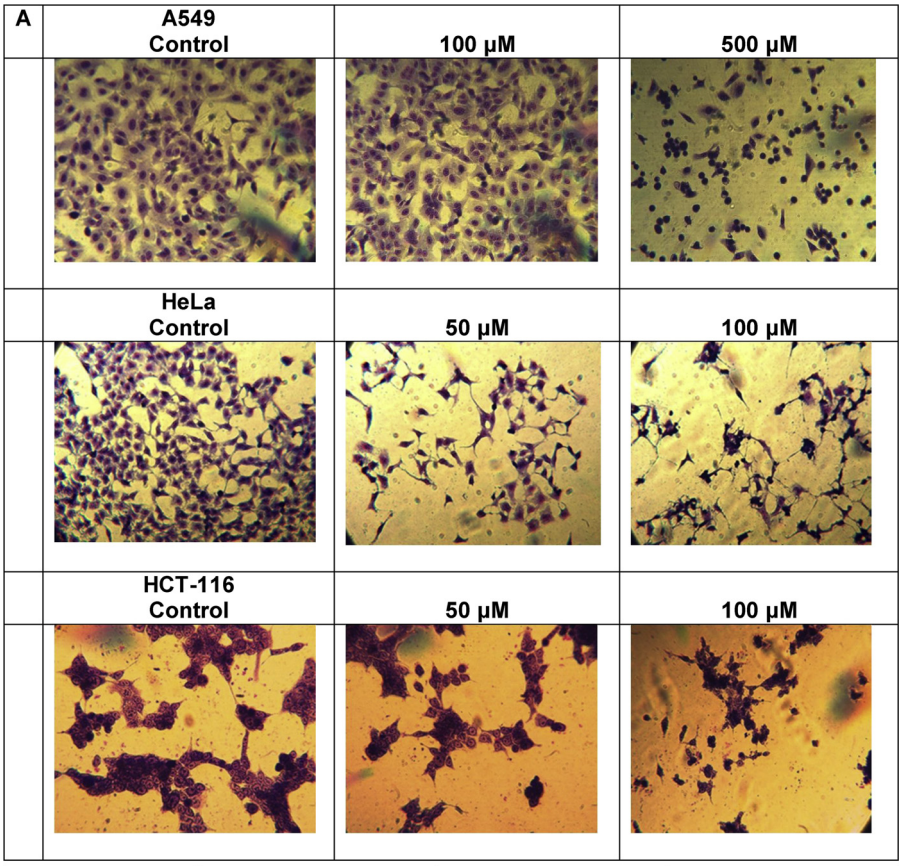


| Scoring | A549 | | | HeLa | | | HCT-116 | | |
|---|---|---|---|---|---|---|---|---|---|
| Cu5HTP, µM | Control | 100 | 500 | Control | 50 | 100 | Control | 50 | 100 |
| Cell shrinkage | - | - | ++++ | - | ++ | ++++ | - | - | ++++ |
| Pyknotic nuclei | - | - | ++++ | - | ++ | ++++ | - | - | ++++ |

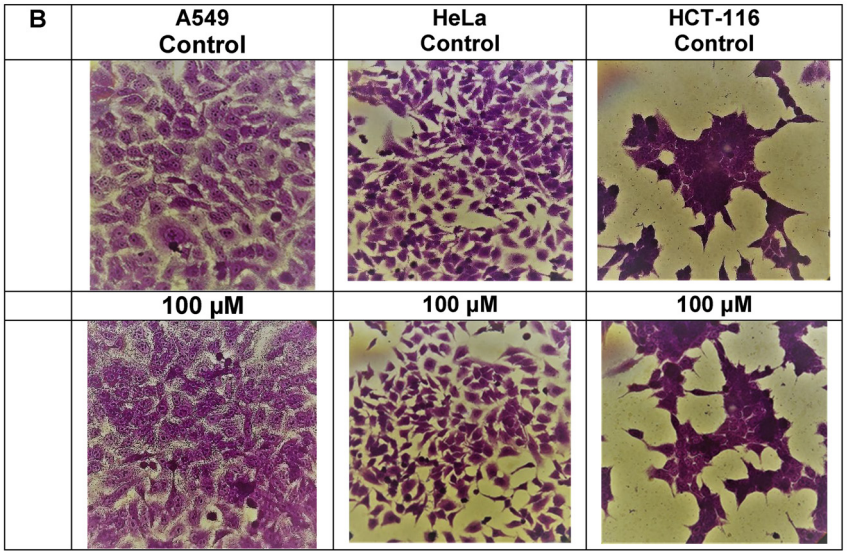


**Fig. 4.** Morphological changes of A549, HeLa and HCT-116 cells after treatment with A) Cu5HTP and B) $CuCl_2$, respectively, for 24 h. Control cells remained untreated and received an equal volume of the solvent. Representative images (100X magnification) by inverted microscope. Fig. 4A includes the scoring of morphological changes: Normal (-), in between normal and mild (+), mild (++), moderate (+++) and sever (++++). This scoring is negative for Fig. 4B ($CuCl_2$ treatment).

not exert toxic effects.

On the other hand, the Ames *Salmonella typhimurium* assay has been used to identify substances that can produce genetic damage that leads to gene mutations. The test uses *Salmonella* strains with preexisting mutations that are not capable to synthesize histidine, and then are not able to grow or form colonies in its absence. Compounds with

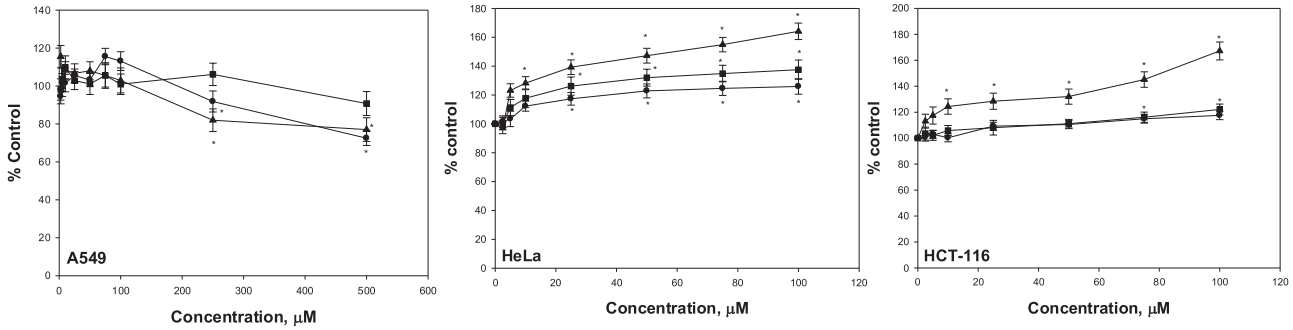


**Fig. 5.** Effects of 5-HTP (circles), Cu5HTP (triangles) and copper(II) cation (squares) on $H_2$DCFDA oxidation to DCF at 24 h. A549, HeLa and HCT-116 cells were incubated at 37 °C in the presence of 10 μM $H_2$DCFDA. The values are expressed as the percentage of the control level and represent the mean ± SEM (n = 15). * significant values in comparison with the control level ($p < 0.05$).

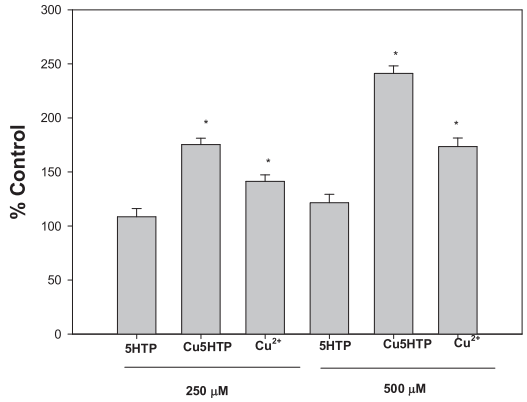


**Fig. 6.** Effects of 5-HTP, Cu5HTP and copper(II) cation on $H_2$DCFDA oxidation to DCF on A549 cell line at 2 h. The values are expressed as the percentage of the control level and represent the mean ± SEM (n = 15). * significant values in comparison with the control level ($p < 0.05$).

mutagenic potential may restore the genes function (reversion assay). Consequently, a positive test indicates that the compound is mutagenic and therefore may act as a carcinogen. A sample was considered positive when the mutagenic index (MI) was equal or greater than 2 for at least one of the tested doses and if it had a reproducible dose-response curve [25]. It can be seen in Table S4 that the $CuCl_2$, 5-HTP and the Cu5HTP complex did not exert mutagenic action on the tested strains. In agreement with our data, the absence of mutagenic activity of $Cu^{2+}$ (as the perchlorate salt) in the Ames test employing *S. typhimurium* TA98 and *S. typhimurium* TA100 (with metabolic activation) was previously reported [51]. The mutagenic index value (lower than 2) in all the cases showed that the tested substances could not induce an increase in the number of revertants. These results indicated that the tested compounds did not induce frameshift mutations (*S. typhimurium* TA98) or base-pair substitution mutations (*S. typhimurium* TA100) at the tested concentrations.

### 3.6. Neuroprotective effects

To assess the effects of glutamate on plasma membrane integrity, LDH quantification in supernatants of treated and untreated cells was employed. As shown in Fig. 7A, exposure to 100 μM glutamate for 15 min induced a significant increase (*ca.* 300%) in LDH release compared to the control untreated cells. No differences of less than 20% were observed with any of the compounds except with the compound Cu5HTP at 0.1 μM which decreased the production of LDH induced by glutamate by 30%. These findings meant a clear neuroprotective improvement against 5HTP and $CuCl_2$.

N-Methyl-D-aspartate (NMDA) receptors produce the activation of specific calcium-dependent signaling cascades which allows the regulation of functional and structural plasticity of individual synapses, dendrites and neurons. The co-agonists Glutamate and glycine must bind the receptor to activate it opening the ion channel. MK801 is a noncompetitive antagonist that blocks the ion channel by binding to allosteric sites and is used to prevent neuronal degeneration caused by N-Methyl-D-aspartate (NMDA). From Fig. 7A it can be seen that MK801 behaves like untreated cells (control cells), which confirmed that the toxicity on cortical neurons was due to the glutamate action [52]. In order to quantify cell number Hoechst 33342 staining was used (Fig. 7B). Glutamate treatment resulted in 45% of mortality in neurons when measured 24 h after exposure. On the other hand the known neuroprotective molecule MK801 prevents OGD-induced mortality by 22%. Glutamate-induced cell death could be also prevented by application of the 5-HTP at 0.1 μM and by application of Cu5HTP at all the concentrations tested. Therefore, compounds supplementation significantly reduced cell death and improved survival of neurons. Again, it was observed a clear neuroprotective improvement of Cu5HTP compound against 5-HTP. No neuroprotection in cell number was observed with the compound $CuCl_2$.

To examine whether glutamate-induced cytotoxicity is mediated by apoptotic processes, caspases 3/7 activation assay was measured (Fig. 7C). Glutamate treatment resulted in a 4.5 fold- increase of caspase 3/7 activation in neurons when measured 24 h after exposure whereas the neuroprotective positive control MK801, prevented OGD-induced apoptosis by 60%. Glutamate induced caspase 3/7 activation could be also prevented by the application of Cu5HTP in all the concentrations tested (0.1, 1 and 10 μM) by 60% while the 5-HTP compound could only protect at the highest tested concentration (10 μM). Therefore, compounds supplementation significantly reduced caspase 3/7 activation and improved survival of neurons. Again, it was observed a clear neuroprotective improvement of Cu5HTP compound against 5-HTP. On the other hand, no neuroprotective effect in caspase 3/7 activation was observed with $CuCl_2$ compound and it was even toxic increasing caspase 3/7 activation at the highest concentrations (1 and 10 μM).

To investigate the ability of the compounds that affects the growth of neurite, a geometric pattern was mainly employed: the neurite average branch length per neuron. Fig. 7D showed that glutamate treatments resulted in a decrease of 55% in neurite outgrowth compared to untreated cells. Glutamate induced neurite outgrowth reduction could be prevented by application of Cu5HTP by 27 and 37% at 0.1 and 1 μM respectively while 5-HTP could only protect at the lowest tested concentration (0.1 μM). Again, it was observed a clear neuroprotective improvement of Cu5HTP compound against 5-HTP. On the other hand, no neuroprotective effect was seen with $CuCl_2$ compound.

Therefore, it the present study, the preventive effects shown by Cu5HTP and 5-HTP against glutamate toxicity are associated with increase of cell number, restoration of caspase 3/7 activity, stabilization of neurite outgrowth and a decrease of LDH secretion. Both compounds

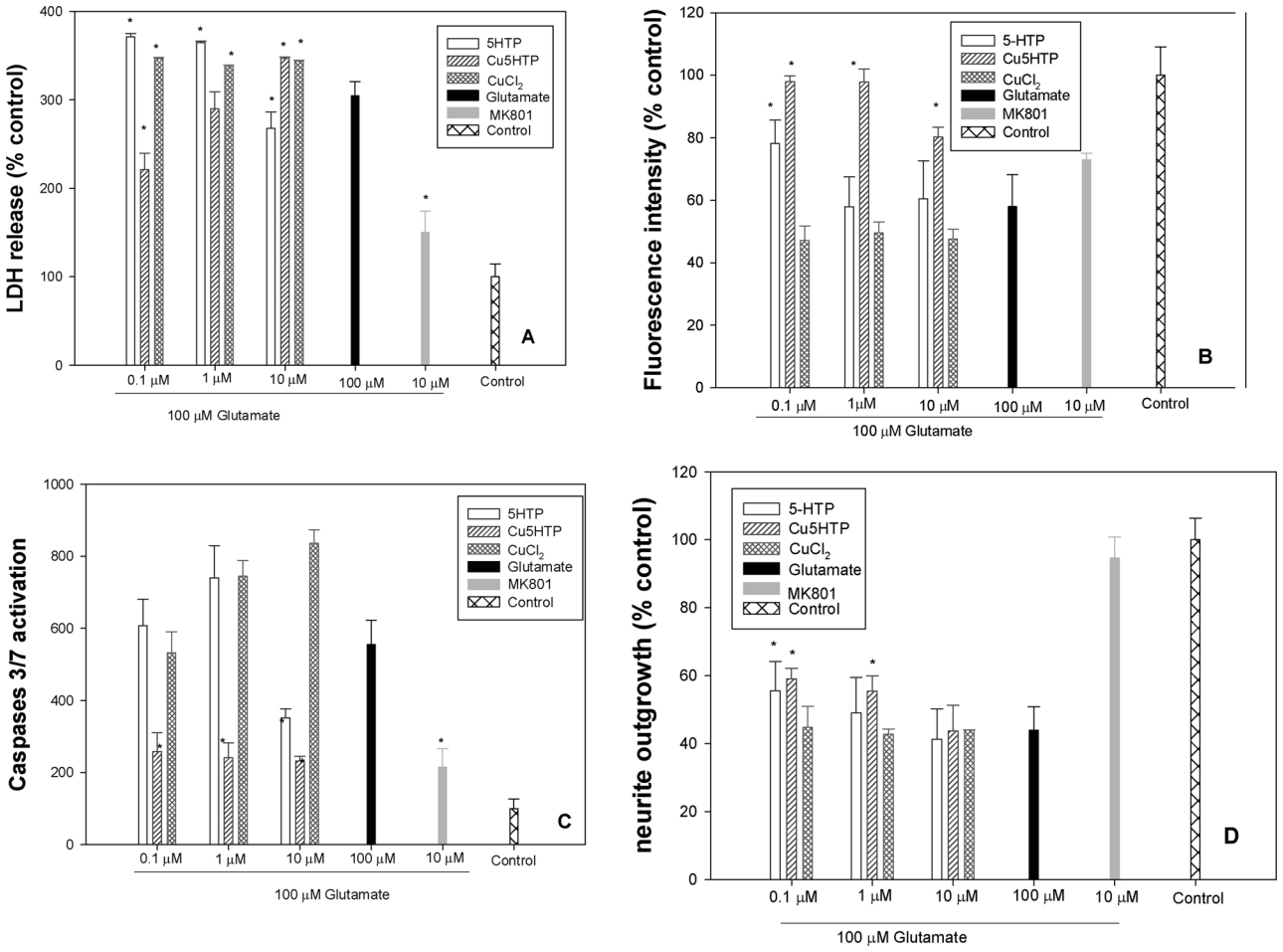


**Fig. 7.** Primary cortical rat neurons were pre-treated with 5-HTP, Cu5HTP and $CuCl_2$ at different concentrations (0.1, 1 and 10 μM) for 1 h. After 48 h, neurons were exposed to 100 μM of glutamate (Glu) for 15 min. The effects of the compounds were quantified by (A), lactate dehydrogenase (LDH) release (B) changes in nuclear morphology (Hoechst-staining) (C) caspases 3/7 activity (apoptosis) (D) neurite outgrowth. 10 μM of MK801 was used as positive control of neuroprotection. The results are expressed as the percentage of the basal level and represent the mean ± the standard error of the mean (SEM) from three separate experiments (n = 9). * significant values in comparison with the control level ($p < 0.05$).

attenuated the toxic effects of glutamate on caspase, cell death, and neurite outgrowth but Cu5HTP compound possessed higher neuroprotective capacity than 5-HTP.

## 4. Discussion

In this paper we have designed and studied a new copper(II) complex with the antioxidant ligand 5-HTP and shown the synthesis and the detailed characterization. Using different spectroscopic techniques we have established the (N,O) chelating nature of the ligand both in solid state and in solution.

In accordance with generalized EPR data of copper(II) bis-aminoacid complexes the calculated EPR parameters help to define the geometric isomerism (cis- or trans-) of the complex. The value of the hyperfine coupling constant obtained from the solution EPR spectrum of Cu5HTP resulted between the values of both type of isomers ($A_{//}$ = 171 and 201 G and $A_{\perp}$ = 16 and 32 G for *trans*-$CuN_2O_2$ and *cis*-$CuN_2O_2$ complexes, respectively [53], but closer to the *trans*- isomer (Fig. 2) indicating that this conformer should be the majority species in solution. These results confirm the findings that correlate the vibrational DFT studies and the experimental FTIR spectra in solid state.

The aminoacid acts as a naturally occurring, endogenous antioxidant in the intertidal sponge *Hymeniacidon heliophila.* This compound is present in the animal in the concentration range of other well-known antioxidants like flavonoids in plants (*ca.* 10 mM). Its antioxidant activity has previously been determined at 10 mM concentration regarding the protection exerted by the compound on human monocytes against UV-induced apoptosis (apoptosis caused by stress oxidative) [2]. Moreover, in the present study it has been determined that 5-HTP showed a good radical-scavenging activity against $ROO^{\cdot}$ and $DPPH^{\cdot}$, but not against superoxide anion and $OH^{\cdot}$ radical (at least at concentrations up to 75 μM). Previous reports showed that hydroxyl radicals were effectively scavenged by the ligand but agree that it has no effect on the superoxide radicals [2] and that the antioxidant effect of the aminoacid may be due to the active hydrogen-donating ability of hydroxyl substitution. In the knowledge that the biological activities of an organic ligand can be increased when coordinated with suitable metal ions, we found that the copper complex behaved as a more potent free radical-scavenging agent enhancing the antioxidant capacity of 5-HTP.

The anticancer effects of the compounds were checked by means of the measurements of the growth inhibitory efficacy in cancer cell lines. The complex Cu5HTP resulted more effective against human cervical (HeLa) and human colon (HCT-116) cancer cell lines than on human lung cancer (A549) cell line. Therapeutic effects of anticancer drugs on tumor cells are associated with various unwished toxic effects on non-tumor cells like hair loss, cardiac anomalies, bone narrow toxicity, nausea and vomiting. Herein we show the lack of toxicity at the tested concentrations for the ligand and its copper complex using different assays: on a non-malignant human lung fibroblast (MRC5) cell line, the

effect against *Artemia Salina* and the Ames test. Hence, their anticancer activity has been correlated well with tumor-specificity (higher cytotoxicity against tumor cells *versus* normal cells).

Non-transformed cells (like MRC-5 cell line) have a lower basal intracellular ROS level, and have a full antioxidant capacity, being less vulnerable to the oxidative stress induced by different compounds in cancer cells. Cancer cells have higher levels of ROS than normal cells and controlled ROS levels exert a pro-survival effect in cancer cells. But, under ROS stress, malignant cells could induce apoptosis or necrosis [54]. It has previously been reported that the pro-oxidant nature of the complexes is manifested mainly in the cancer cells, the mechanism of which is still unclear.

The observation of elevated ROS in the cell lines in the presence of Cu5HTP is an evidence of a mechanism of action involving oxidative stress. Notably, the compound displayed the highest activity by generation of the highest cellular level of ROS *in vitro* and hence, the cytotoxicity of the complex resulted greater than either the 5-HTP ligand or free Cu(II). This may indicate that the ligand plays a role in enabling the copper centers to effectively generate elevated levels of toxic ROS, giving rise to cell death.

As it is known that 5-HTP is involved in the biosynthesis of the neurotransmitter Serotonin and that glutamate excitotoxicity is involved in many neurodegenerative diseases we have also studied the neuroprotection of the compounds on neuronal injury in cell culture after exposure to glutamate. LDH is a ubiquitous cytoplasmic oxidoreductase which is used as biochemical index of neuronal injury [55]. The lowest tested concentration of the complex and the highest of the ligand decreased the LDH release which implies that the compounds protected the cells against glutamate-induced cytotoxicity, being Cu5HTP more effective than 5-HTP. The results are in agreement with those obtained by the Hoechst assay. It is known that neuronal cell death induced by glutamate can occur through the disruption of intracellular calcium homeostasis followed by mitochondrial uncoupling and activation of the intrinsic mitochondrial apoptosis pathway by triggering caspases activation [56]. In this work, we have shown that Cu5HTP (at the three tested concentrations) decreased caspase 3/7 activity like the NMDA receptor antagonist, MK801. The aminoacid 5-HTP only showed this effect at 10 μM concentration. The current results suggest that Cu5HTP and to a lesser extent 5-HTP, exerted neuroprotection against Glu-induced excitotoxicity in primary cultures of cortical neurons, due in part to the to its anti-apoptotic effect, like the aminoacid taurine [15]. After an injury, the central nervous system of adult mammals has limited capacity to regenerate due to insufficient stimulation of a growth response following injury, the release of growth inhibitory molecules from myelin and the formation of scar tissue at the site of injury [57]. Neurite outgrowth is a process involved in the brain development and it is related to the synaptic structure, characteristics of information transmission efficiency and neuronal synaptic plasticity [58]. In addition to neuroprotection, for the damaged brain to restore normal physiological functions, the reorganization of the lost neuronal network is indispensable. Taking into account that the complex induced neurite extension in cortical neurons and exerted preventive effects demonstrated by the decrease of the LDH release and the increase in the cell number, through a caspase dependent mechanism, Cu5HTP could be considered as a potential neuroprotective agent against glutamate induced cell-death. While the biometal did not exert protective effects, the ligand showed protective effects at some of the tested concentrations.

## 5. Conclusions

The 5-hydroxytryptophan Copper(II) complex (Cu5HTP) has been synthesized and characterized by elemental analysis, thermogravimetric analysis, spectroscopic techniques, and computational studies. The conformational investigations of the solid complex suggest the coexistence of two conformers of Cu5HTP with *cis*- and *trans*-arrangements of the amino acids in the equatorial plane (optimized in gas phase at B3LYP/6-311G** theory level) at room temperature. The Cu5HTP1 complex (with *trans*- configuration) is the most stable conformer. The biological activities of the metal complex resulted enhanced with respect to the ligand. Copper(II) complexation enhances the antioxidant properties of 5-HTP. The complex showed improved anticancer effects by means of a pro-oxidant mechanism in cancer cells. The neuroprotective action of the complex on neuronal injury in cell culture after exposure to glutamate resulted more effective than that of 5-HTP. The ligand and the complex did not exert toxic effects against *Artemia salina* and did not behave as mutagenic agents indicating that these compounds have the potential to act as effective antioxidant drugs. In this context, we can conclude that some biological properties have been modified upon complexation with copper(II) and this complexation may provide a promising strategy for the development of novel and more secure anticancer and neuroprotective drugs with antioxidant properties.

## Conflict of interest

There was no conflict of interest among any of the authors.

## Acknowledgements

This work was supported by UNLP, CICPBA, UNCAus, CONICET, CAI + DUNL, PIP (0611) and ANPCyT (PICT 2016-1814, 2014-1742), Argentina. EGF, LGN and NBO are research fellows of CONICET. PAMW is a research fellow of CICPBA, Argentina. JJMM and ALP are fellowship holders from CONICET.

## Appendix A. Supplementary data

Supplementary material related to this article can be found, in the online version, at doi:https://doi.org/10.1016/j.biopha.2018.12.098.

## References

[1] R. Hara, K. Kino, Enhanced synthesis of 5-hydroxy-l-tryptophan through tetrahydropterin regeneration, AMB Express 3 (2013) 1–7.
[2] N. Lysek, R. Kinscherf, R. Claus, T. Lindel, L-5-hydroxytryptophan: antioxidant and anti-apoptotic principle of the intertidal sponge Hymeniacidon heliophila, Z. Naturforsch. 58c (2003) 568–572.
[3] J.F. Collins, Copper: basic physiological and nutritional aspects, Molecular, Genetic, and Nutritional Aspects of Major and Trace Minerals, Academic Press, Boston, 2017, pp. 69–83 Chap. 7ISBN 9780128021682.
[4] A. Gupte, R.J. Mumper, Anti-tumour treatment. Elevated copper and oxidative stress in cancer cells as a target for cancer treatment, Cancer Treat. Rev. 35 (2009) 32–46.
[5] I. Iakovidis, I. Delimaris, S.M. Piperakis, Copper and its complexes in medicine: a biochemical approach, Res. Mol. Biol. Int. (2011) 1–13, https://doi.org/10.4061/2011/594529.
[6] X. Shen, M. Yang, S.A. Tomellini, Indirect fluorescence detection of amino sugars with the use of copper complexes of tryptophan and its analogues following high-performance liquid chromatographic separation, J. Chromatogr. A 1072 (2005) 273–277.
[7] O.A. Weber, V. Simeon, Tryptamine, 5-hydroxytryptamine and 5-hydroxytryptophan complexes of proton and some divalent metal ions, Inorg. Nucl. Chem. 33 (1971) 2097–2101.
[8] R. Pfragner, R.I. Freshney (Eds.), Culture of Human Tumor Cells, John Wiley & Sons, 2004.
[9] T.A. Yacoubian, Neurodegenerative disorders: Why do we need new therapies? in: A. Adejare (Ed.), Drug Discovery Approaches for the Treatment of Neurodegenerative Disorders. Alzheimer's Disease, Academic Press, 2016, pp. 1–16 Chap 1.
[10] T.C. Birdsall, 5-hydroxytryptophan: a clinically-effective serotonin precursor, Altern. Med. Rev. 3 (1998) 271–280.
[11] L.P. Mark, R.W. Prost, J.L. Ulmer, M.M. Smith, D.L. Daniels, J.M. Strottmann, W.D. Brown, L. Hacein-Bey, Pictorial review of glutamate excitotoxicity: fundamental concepts for neuroimaging, AJNR Am. J. Neuroradiol. 22 (2001) 1813–1824.
[12] X. Dong, Y. Wang, Z. Qin, Molecular mechanisms of excitotoxicity and their relevance to pathogenesis of neurodegenerative diseases, Acta Pharmacol. Sin. 30 (2009) 379–387.
[13] Y.S. Ho, M.S. Yu, S.Y. Yik, K.F. So, W.H. Yuen, R.C.C. Chang, Polysaccharides from

wolfberry antagonizes glutamate excitotoxicity in rat cortical neurons, Cell. Mol. Neurobiol. 29 (2009) 1233–1244.
[14] P. Mehta, W. Kaye, J. Raymond, R. Wu, T. Larson, R. Punjani, D. Heller, J. Cohen, T. Peters, O. Muravov, K. Horton, Prevalence of amyotrophic lateral sclerosis - United States, 2014, Morb. Mortal. Wkly. Rep. 67 (2018) 216–218.
[15] J.E. Jeong, T.Y. Kim, H.J. Park, K.H. Lee, K.H. Lee, E.J. Choi, J.K. Kim, H.L. Chung, E.S. Seo, W.T. Kim, Taurine exerts neuroprotective effects via anti-apoptosis in hypoxic-ischemic brain injury in neonatal rats, Korean J. Pediatrics 52 (2009) 1337–1347.
[16] S. Stoll, A. Schweiger, EasySpin, a comprehensive software package for spectral simulation and analysis in EPR, J. Magn. Reson. 178 (2006) 42–55.
[17] R.G. Parr, W. Yang, Density Functional Theory of Atoms, Molecules, Oxford University Press, Clarendon Press, Oxford; New York, 1989.
[18] M.J. Frisch, G.W. Trucks, H.B. Schlegel, G.E. Scuseria, M.A. Robb, J.R. Cheeseman, G. Scalmani, V. Barone, B. Mennucci, G.A. Petersson, H. Nakatsuji, M. Caricato, X. Li, H.P. Hratchian, A.F. Izmaylov, J. Bloino, G. Zheng, J.L. Sonnenberg, M. Hada, M. Ehara, K. Toyota, R. Fukuda, J. Hasegawa, M. Ishida, T. Nakajima, Y. Honda, O. Kitao, H. Nakai, T. Vreven, J.A. Montgomery Jr., J.E. Peralta, F. Ogliaro, M. Bearpark, J.J. Heyd, E. Brothers, K.N. Kudin, V.N. Staroverov, T. Keith, R. Kobayashi, J. Normand, K. Raghavachari, A. Rendell, J.C. Burant, S.S. Iyengar, J. Tomasi, M. Cossi, N. Rega, J.M. Millam, M. Klene, J.E. Knox, J.B. Cross, V. Bakken, C. Adamo, J. Jaramillo, R. Gomperts, R.E. Stratmann, O. Yazyev, A.J. Austin, R. Cammi, C. Pomelli, J.W. Ochterski, R.L. Martin, K. Morokuma, V.G. Zakrzewski, G.A. Voth, P. Salvador, J.J. Dannenberg, S. Dapprich, A.D. Daniels, O. Farkas, J.B. Foresman, J.V. Ortiz, J. Cioslowski, D.J. Fox, Gaussian 09, Revision B.01, Gaussian, Inc., Wallingford CT, 2010.
[19] A.D. Becke, Density functional thermochemistry. III. The role of exact exchange, J. Chem. Phys. 98 (1993) 5648–5652.
[20] R. Krishnan, J.S. Binkley, R. Seeger, J.A. Pople, Self-consistent molecular orbital methods. XX. A basis set for correlated wave functions, J. Chem. Phys. 72 (1980) 650–654.
[21] A. Wakahara, M. Kido, T. Fujiwara, K. Tomita, Structural studies of tryptophan metabolites by X-ray diffraction method. I. The crystal and molecular structure of 5-Hydroxy-DL-tryptophan, Bull. Chem. Soc. Japan 46 (1973) 2475–2480.
[22] M.H. Jamróz, Vibrational Energy Distribution Analysis, VEDA 4.0 Program, Warsaw 2004-2010.
[23] J.J. Martínez Medina, L.G. Naso, A.L. Pérez, A. Rizzi, N.B. Okulik, E.G. Ferrer, P.A.M. Williams, Apigenin oxidovanadium(IV) catión interactions. Synthesis, spectral, bovine serum albumin binding, antioxidant and anticancer studies, J. Photochem. Photobiol. A: Chem. 344 (2017) 84–100.
[24] L. Lewan, M. Andersson, P. Morales-Gomez, Use of Artemia salina in toxicity testing, Altern. Lab. Anim. 20 (1992) 297–301.
[25] D.M. Maron, B.N. Ames, Revised methods for the Salmonella mutagenicity test, Mutat. Res. 113 (1983) 173–215.
[26] E. Ituen, O. Akaranta, A. James, Electrochemical and anticorrosion properties of 5-hydroxytryptophan on mild steel in a simulated well-acidizing fluid, J. Taibah Univ. Sci. 11 (2017) 788–800.
[27] X. Cao, Infrared spectral, structural, and conformational studies of zwitterionic L-Tryptophan, G. Fischer, J. Phys. Chem. A 103 (1999) 9995–10003.
[28] C.C. Wagner, E.J. Baran, Spectroscopic and magnetic behaviour of the copper(II) complex of L-Tryptophan, Acta Farm. Bonaerense 23 (2004) 339–342.
[29] A. Stanila, A. Marcu, D. Rusu, M. Rusu, L. David, Spectroscopic studies of some copper(II) complexes with amino acids, J. Mol. Struct. 834–836 (2007) 364–368.
[30] G.B. Deacon, R.J. Phillips, Relationships between the carbon-oxygen stretching frequencies of carboxylato complexes and the type of carboxylate coordination, Coord. Chem. Rev. 33 (1980) 227–250.
[31] E. Garribba, G. Micera, The determination of the geometry of Cu(II) complexes: an EPR spectroscopy experiment, J. Chem. Ed. 83 (2006) 1229–1232.
[32] N.I. Neuman, V.G. Franco, F.M. Ferroni, R. Baggio, M.C.G. Passeggi, A.C. Rizzi, C.D. Brondino, Single crystal EPR of the mixed-ligand complex of copper(II) with l-glutamic acid and 1,10-phenanthroline: a study on the narrowing of the hyperfine structure by exchange, J. Phys. Chem. A 116 (2012) 12314–12320.
[33] J.P. Merrick, D. Moran, L. Radom, An evaluation of harmonic vibrational frequency scale factors, J. Phys. Chem. A 111 (2007) 11683–11700.
[34] E. Prenestia, P.G. Daniele, M. Prencipe, G. Ostacoli, Spectrum–structure correlation for visible absorption spectra of copper(II) complexes in aqueous solution, Polyhedron 18 (1999) 3233–3241.
[35] A.C. Rizzi, N.I. Neuman, P.J. González, C.D. Brondino, EPR as a tool for study of isolated and coupled paramagnetic centers in coordination compounds and macromolecules of biological interest, Eur. J. Inorg. Chem. 2016 (2016) 192–207.
[36] J. Peisach, W.E. Blumberg, Structural implications derived from the analysis of electron paramagnetic resonance spectra of natural and artificial copper proteins, Arch. Biochem. Biophys. 165 (1974) 691–708.
[37] N.V. Nagy, T. Szabó -Plánka, A. Rockenbauer, G. Peintler, I. Nagypál, L. Korecz, Great structural variety of complexes in copper(II)-oligoglycine systems: micro-speciation and coordination modes as studied by the two-dimensional simulation of Electron paramagnetic resonance spectra, J. Am. Chem. Soc. 125 (2003) 5227–5235.
[38] W.J. Geary, The use of conductivity measurements in organic solvents for the characterization of coordination compounds, Coord. Chem. Rev. 7 (1981) 81–122.
[39] M.S. Islas, T. Rojo, L. Lezama, M. Griera Merino, M.A. Cortes, M. Rodriguez Puyol, E.G. Ferrer, P.A.M. Williams, Improvement of the antihypertensive capacity of candesartan and trityl candesartan by their SOD mimetic copper(II) complexes, J. Inorg. Biochem. 123 (2013) 23–33.
[40] P. Siddhuraju, K. Becker, Studies on antioxidant activities of mucuna seed (*Mucuna pruriens* var *utilis*) extract and various non-protein amino/imino acids through *in vitro* models, J. Sci. Food Agric. 83 (2003) 1517–1524.
[41] H. Khalid, M. Hanif, M.A. Hashmi, T. Mahmood, K. Ayub, M.M. Mehboob, Copper complexes of bioactive ligands with superoxide dismutase activity, Mini-Rev. Med. Chem 13 (2013) 1944–1956.
[42] M. Fatfat, R.A. Merhi, O. Rahal, D. Stoyanovsky, A. Zaki, H. Haidar, V.E. Kagan, H. Gali-Muhtasib, K. Machaca, Copper chelation selectively kills colon cancer cells through redox cycling and generation of reactive oxygen species, BMC Cancer 14 (2014) 527–539.
[43] J.G. Da Silva, P.R. da Costa, R.G. dos Santos, H. Beraldo, ROS-mediated cytotoxic effect of copper(II) hydrazone complexes against human glioma cells, Molecules 19 (2014) 17202–17220.
[44] Z. Ren, H. Yu, J. Li, J. Shen, W. Du, Suitable parameter choice on quantitative morphology of A549 cell in epithelial-mesenchymal transition, Biosci. Rep. 35 (2015) 1–7.
[45] I. Martínez-Ramos, A. Maya-Mendoza, P. Gariglio, A. Aranda-Anzaldo, Global but stable change in HeLa cell morphology induces reorganization of DNA structural loop domains within the cell nucleus, J. Cell. Biochem. 96 (2005) 79–88.
[46] J. Groden, G. Joslyn, W. Samowitz, D. Jones, N. Bhattacharyya, L. Spirio, A. Thilveris, M. Robertson, S. Egan, M. Meuth, R. White, Response of Colon Cancer cell lines to the introduction of APC, a colon-specific tumor suppressor gene, Cancer Res. 55 (1995) 1531–1539.
[47] S. Pervaiz, M. Clément, Tumor intracellular redox status and drug resistance-serendipity or a causal relationship? Curr. Pharm. Des. 10 (2004) 1969–1977.
[48] P. Schumacker, Reactive oxygen species in cancer: a dance with the devil, Cancer Cell 27 (2015) 156–157.
[49] A. Lagarto Parra, R. Silva Yhebra, I. Guerra Sardiñas, L. Iglesias Buela, Comparative study of the assay of *Artemia salina L.* and the estimate of the medium lethal dose (LD50 value) in mice, to determine oral acute toxicity of plant extracts, Phytomedicine 8 (2001) 395–400.
[50] V. Kokkali, I. Katramados, J.D. Newman, Monitoring the effect of metal ions on the mobility of *Artemia salina* nauplii, Biosensors 1 (2011) 36–45.
[51] B. Duff, V.R. Thangella, B.S. Creaven, M. Walsh, D.A. Egan, Anti-cancer activity and mutagenic potential of novel copper(II) quinolinone Schiff base complexes in hepatocarcinoma cells, Eur. J. Pharmacol. 689 (2012) 45–55.
[52] P. Kovacic, R. Somanathan, Clinical physiology and mechanism of dizocilpine (MK-801): electron transfer, radicals, redox metabolites and bioactivity, Oxid. Med. Cell. Longev. 3 (2010) 13–22.
[53] M.S. Bukharov, V.G. Shtyrlin, A.S. Mukhtarov, G.V. Mamin, S. Stapf, C. Mattea, A.A. Krutikov, A.N. Il'ina, N.Y. Serov, Study of structural and dynamic characteristics of copper(II) amino acid complexes in solutions by combined EPR and NMR relaxation methods, Phys. Chem. Chem. Phys. 16 (2014) 9411–9421.
[54] L. Gibellini, M. Pinti, M. Nasi, S. De Biasi, E. Roat, L. Bertoncelli, A. Cossarizza, Interfering with ROS metabolism in cancer cells: the potential role of quercetin, Cancers 2 (2010) 1288–1311, https://doi.org/10.3390/cancers2021288.
[55] J.Y. Koh, D.W. Choi, Quantitative determination of glutamate mediated cortical neuronal injury in cell culture by lactate dehydrogenase efflux assay, J. Neurosci. Meth. 20 (1987) 83–90.
[56] N.A. Rivero-Segura, E. Flores-Soto, S. García de la Cadena, I. Coronado-Mares, J.C. Gomez-Verjan, D.G. Ferreira, E. Alejandra Cabrera-Reyes, L.V. Lopes, L. Massieu, M. Cerbón, Prolactin-induced neuroprotection against glutamate excitotoxicity is mediated by the reduction of $[Ca^{2+}]$i overload and NF-κB activation, PLoS One 12 (2017) e0176910.
[57] P.J. Mitchell, J.C. Hanson, A.T. Quets-Nguyen, M. Bergeron, R.C. Smith, A quantitative method for analysis of in vitro neurite outgrowth, J. Neurosci. Meth. 164 (2007) 350–362.
[58] F. Hong, L. Sheng, Y. Zeb, J. Hong, Y. Zhou, L. Wang, D. Liu, X. Yu, B. Xu, X. Zhao, X. Ze, Suppression of neurite outgrowth of primary cultured hippocampal neurons is involved in impairment of glutamate metabolism and NMDA receptor function caused by nanoparticulate $TiO_2$, Biomaterials 53 (2015) 76–85.